

# Characteristics and Efficiency of Heat Transfer for Natural Convection by Ag-CuO/H<sub>2</sub>O Hybrid Nanofluid Inside a Square Cavity with Corrugated Walls

Razik Benderradji<sup>1</sup>, Meryem Brahimi<sup>1,2</sup>, Hamza Goudmi<sup>3</sup>

<sup>1</sup>Department of Physics, Faculty of Sciences, University of M'sila, Algeria.

<sup>2</sup>Laboratory of Materials and Renewable Energy (LMER), University of M'sila, Algeria.

<sup>3</sup>Department of Mechanical Engineering, Faculty of Sciences and Technology, University of Bordj Bou Arreridj, El-Anasser 34030, Algeria.

## Abstract

This study presents a parametric numerical investigation of laminar natural convection and heat transfer in a cavity with opposite sinusoidal wavy walls, filled with hybrid Ag-CuO/water nanofluid. The vertical walls of the cavity are maintained at distinct hot and cold temperatures, while the upper and lower boundaries are thermally insulated. The study examines the effects of key factors, including the sinusoidal wall shape, nanoparticle volume fractions ( $0\% \leq \phi \leq 6\%$ ), and Rayleigh numbers ( $10^3 \leq Ra \leq 10^6$ ). A finite volume discretization method, using the SIMPLE algorithm, is employed to solve the governing equations, with Ansys Fluent software ensuring quadratic accuracy. Mesh independence is confirmed with a  $200 \times 200$  mesh, and code validation is performed through comparison with previous studies. Results indicate that increasing the nanoparticle volume fraction enhances heat transfer within the cavity. Additionally, the Rayleigh number significantly influences the heat transfer mode, with higher Ra values promoting stronger convective activity. Detailed analysis of temperature and velocity profiles, along with Nusselt number variations, highlights the impact of nanoparticle concentrations and Rayleigh numbers. The wavy wall geometry improves fluid mixing and thermal boundary layer interaction, leading to enhanced heat dissipation. These findings underscore the potential of hybrid nanofluids and wavy wall designs to optimize heat transfer in engineering systems.

**Keywords:** Wavy Wall Enclosure, Natural Convection, Hybrid nanofluid, Heat transfer, Rayleigh number.

## 1. Introduction

Thermal transfer is a discipline aimed at understanding the energy transfer between molecules or particles of matter at different temperatures. Governed by a combination of physical laws and empirical relationships derived from experimentation, this process is ubiquitous in various industrial (thermal and electric engines, fuel and gas power plants, etc.) and domestic (heating systems) contexts. The specialized literature in this field generally recognizes three distinct modes of heat transmission: conduction, convection, and radiation.

Enhancing heat transfer through convection is the primary goal of numerous studies. To achieve this objective, many researchers have undertaken a variety of numerical and experimental trials, focusing on describing the phenomena governing convection, the influence of system nature (especially geometry), and the properties of involved fluids (physicochemical properties). These efforts have mainly addressed the macroscopic, and sometimes microscopic, aspects of the process. A wide range of methods have been employed recently to increase the velocity of heat transfer in order to reach a desirable degree of thermal efficiency. Enhancing thermal

Corresponding author: Razik Benderradji ([razik.benderradji@univ-msila.dz](mailto:razik.benderradji@univ-msila.dz))

Received: 21 July 2024; Revised: 20 September 2024; Accepted: 26 September 2024; Published: 1 October 2024

© 2024 The Author(s). This work is licensed under a Creative Commons Attribution 4.0 International License

conductivity is one approach to achieve this. Several attempts have been made to enhance the thermal characteristics of traditional heat transfer fluids by dispersing high thermal conductivity solid particles in the coolant. The first to demonstrate that raising the volume proportion of solid particles in a mixture of solid and liquid could enhance its thermal conductivity was Maxwell [1, 2]. Large particles, however, can lead to a number of bothersome issues, like large particles sedimenting in the base fluid. As a result, a brand-new class of fluid called as nanofluid has been created to enhance thermal conductivity and suspension stability. The benefit of employing nanoparticles scattered throughout a base fluid in various thermal regimes to increase the rate of heat transfer was demonstrated by Choi [3]. According to Eastman et al. [4], the thermal conductivity rose by 40% at a volume concentration of 0.3% of copper nanoparticles dissolved in ethylene glycol. A basic fluid with suspended nanoscale particles of a single type of material is referred to as a "nanofluid" in almost all research published to date in the field of nanofluids. They looked explored how the size, shape, concentration, and composition of nanoparticles affected the thermophysical characteristics of nanofluids and how they affected the characteristics of pressure drop and heat transmission. But lately, a study on nanofluids was conducted experimentally with two different kinds of nanoparticles dispersed concurrently in a base fluid known as "hybrid nanofluid" [5]. The creation of two distinct types of nanoparticles scattered throughout the base fluid is the key component of hybrid nanofluids. Consequently, when particle materials are chosen carefully, they can balance out each other's good qualities and cover up a single material's flaws. For instance,  $\text{Al}_2\text{O}_3$  has less heat conductivity than metal nanoparticles, but alumina, a ceramic substance, has some advantageous qualities such high stability and chemical inertness. High heat conductivity is exhibited by metal nanoparticles such as copper, zinc, aluminum, and others. However, because of their stability and reactivity, metal nanoparticles are not as useful in nanofluidic applications. These features of metallic and non-metallic nanoparticles suggest that adding metallic nanoparticles, such copper, to a nanofluid containing  $\text{Al}_2\text{O}_3$  nanoparticles could enhance the mixture's thermophysical characteristics. Conducting an experimental investigation on the production of hybrid nanofluids of  $\text{Al}_2\text{O}_3$ -Cu and water by Suresh et al. [5]. They employed a thermomechanical

technique (a two-step procedure) to produce the stable hybrid nanofluid. The  $\text{Al}_2\text{O}_3$ -Cu/water hybrid nanofluid was created by adding copper nanoparticles to the  $\text{Al}_2\text{O}_3$ /water nanofluid at various volume concentrations, including 0.1, 0.33, 0.75, 1, and 2%. Given the aforementioned benefits of hybrid nanofluids, it is obvious that this cutting-edge fluid will be essential to the development of nanofluidics in the future. As a result, researchers are increasingly drawn to investigate hybrid nanofluids and how they affect pressure and heat transmission. qualities of projection. Due to its numerous applications in nuclear power, duplex windows, building heating and cooling, solar collectors, electronic refrigeration, and microelectromechanical systems (MEMS), natural convection heat transfer is a significant phenomenon in engineering systems [6–8].

Therefore, to guarantee the effective operation of varied heat transfer equipment, it is required to examine the thermal and hydrodynamic behavior of different shapes of heat transfer surfaces. Natural laminar convection in 2D packages is a well-studied problem in several literatures. The majority of this study (see, for example, [9–11]) has been on the topic of heat transmission via natural convection in corrugated-surfaced containers. In a square enclosure with V-shaped undulating vertical walls, Ali and Hussein [12] investigated the impact of ripple frequencies on heat transmission and natural convection flow characteristics. Numerous studies have been conducted on this topic in addition to standard geometric shapes like the square and rectangle. Because corrugated wall enclosures are used in numerous engineering challenges including technical design requirements, they are mentioned in literature [13]. Numerous industrial and engineering uses for natural convection in a corrugated enclosure exist, including double wall thermal insulation, subterranean cable networks, and microelectronic device cooling [14]. As a result, numerous researchers have published theoretical and experimental results on this geometry because of the practical significance of flow and heat transfer in wavy geometry (e.g., [15–17]). A numerical investigation of static magnetic convection in a sinusoidal corrugated enclosure with a heat source on the bottom wall was conducted by Saha [18]. It shown that the average Nusselt number dropped as the heat source's surface area rose, suggesting that the heat source's size significantly affects the rate of heat transmission. Additionally, in the

geometry given by Saha [18], Hussein et al. [19] conducted a numerical examination of the impact of tilt angles on natural convection. According to their findings, the Nusselt number first rises with higher tilt degrees before falling for all Hartmann number values.

In recent years, advanced studies have increasingly focused on the dynamics of blood flow in stenosed arteries and the impact of nanoparticles on fluid behavior. For instance, research has explored the complex interactions of electro-magnetohydrodynamics in human blood flow using hybrid nanofluids like Cu and CuO, which enhance thermal conductivity and influence viscosity to improve flow characteristics, Shankar et al. [20]. Additionally, the study of heat and mass transfer in Casson nanofluids under double diffusive convection has gained attention for industrial micro-pumping applications, Bathmanaban et al. [21]. Computational models for bio-inspired membrane-based pumping systems in medical applications have also advanced, illustrating how induced magnetic fields affect micro-scale transport phenomena in MRI and electromagnetic therapy, Bhandari et al. [22]. Finally, flow models of Bingham plastic fluids through porous media have contributed to the design of micro-valveless pumps for diagnostic and therapeutic use, Kumar et al. [23].

This study addresses significant gaps in the literature by examining the combined effects of hybrid nanofluids and complex geometries, specifically sinusoidal corrugated enclosures, on heat transfer performance. Despite numerous studies on nanofluids and geometric shapes individually, the interplay between nanoparticle concentration, geometric configurations, and their impact on natural convection remains underexplored. This research will systematically analyze how varying nanoparticle concentrations and Rayleigh numbers influence heat transfer in such enclosures and provide new insights into optimizing thermal performance in complex systems. The study focuses on two main aspects: the effects of nanoparticle concentration and Rayleigh numbers, and the influence of wall geometry.

## 2. Computational Model

### 2.1. Configuration

Figure 1 depicts the examined geometric configuration, emphasizing the principal geometric

characteristics. The cavity comprises two vertical sinusoidal walls and two flat horizontal walls, with dimensions  $L$  and  $H$ , respectively. The left sinusoidal wavy sidewall heats the cavity isothermally at temperature ( $T_c$ ), while the right sinusoidal wavy sidewall cools it at temperature ( $T_f$ ). The following equation characterizes the sinusoidal wave surfaces:  $x = \pm L \sin^2(\frac{n\pi y}{H})$ . We presume thermal insulation for the remaining walls (superior and inferior).

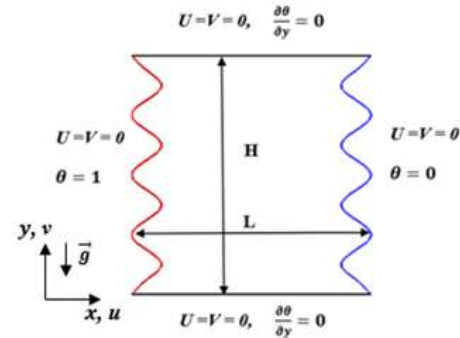


**Figure 1.** The physical scheme of the problem and the boundary conditions.

The flow is assumed to be Newtonian and incompressible in a steady laminar regime in a state of thermal equilibrium. According to the Boussinesq approximations, the density variation is neglected everywhere, except in the buoyancy term. The thermophysical properties with which we will work are shown in Table 1.

**Table 1.** Thermophysical properties of water and nanoparticles with  $T=300$  °K. (Sharma et al [24]).

Physical properties	Unit	H <sub>2</sub> O	Ag	CuO
$\rho$	( $kg \cdot m^{-3}$ )	997.1	10500	6320
$C_p$	( $J \cdot kg^{-1} \cdot K^{-1}$ )	4179	235	531.8
$K$	( $W \cdot m^{-1} \cdot K^{-1}$ )	0.613	429	76.5
$\mu$	( $Kg \cdot m^{-1} \cdot K^{-1}$ )	0.001002	—	—

### 2.2. Governing equations

In this study, we investigate a steady-state, incompressible flow inside a sinusoidal cavity filled with a hybrid nanofluid consisting of water and Ag and CuO nanoparticles. Furthermore, the Navier-Stokes equations, a well-established set of equations in fluid mechanics,

incorporating the Boussinesq approximation, are presented below:

$$\frac{\partial U}{\partial x} + \frac{\partial V}{\partial y} = 0 \quad (1)$$

$$u \frac{\partial u}{\partial x} + v \frac{\partial u}{\partial y} = \frac{1}{\rho_{hnf}} \left( -\frac{\partial p}{\partial x} + \mu_{hnf} \left( \frac{\partial^2 u}{\partial x^2} + \frac{\partial^2 u}{\partial y^2} \right) \right) \quad (2)$$

$$u \frac{\partial v}{\partial x} + v \frac{\partial v}{\partial y} = \frac{1}{\rho_{hnf}} \left[ -\frac{\partial p}{\partial y} + \mu_{hnf} \left( \frac{\partial^2 v}{\partial x^2} + \frac{\partial^2 v}{\partial y^2} \right) + (\rho\beta)_{hnf} g(T - T_c) \right] \quad (3)$$

$$u \frac{\partial T}{\partial x} + V \frac{\partial T}{\partial y} = \alpha_{hn} \left( \frac{\partial^2 T}{\partial x^2} + \frac{\partial^2 T}{\partial y^2} \right) \quad (4)$$

The properties of the hybrid nanofluid are calculated according to the following formulas:

The thermal diffusivity of nanofluid is:

$$\alpha_{nf} = \frac{k_{nf}}{(\rho C_p)_{nf}} \quad (5)$$

The density of a hybrid nanofluid is: (Ghalambaz et al. [25]), (Mabood, Yusuf et al [26])

$$\rho_{hnf} = (1 - \varphi_{hnp})\rho_f + \varphi_1\rho_1 + \varphi_2\rho_2 \quad (6)$$

The heat capacity of a hybrid nanofluid is: (Ghalambaz et al. [25]), (Mabood, Yusuf et al [26])

$$(\rho C_p)_{hn} = (1 - \varphi_{hn})(\rho C_p)_f + \varphi_1(\rho C_p)_1 + \varphi_2(\rho C_p)_2 \quad (7)$$

The coefficient of thermal expansion of hybrid nanofluid can be determined by: (Ghalambaz et al., 2019 [25])

$$(\rho\beta)_{hn} = (1 - \varphi_{hn})(\rho\beta)_f + \varphi_1(\rho\beta)_1 + \varphi_2(\rho\beta)_2 \quad (8)$$

According to Maxwell's model, the thermal conductivity of hybrid nanofluid is: (Mabood et al [26])

$$\frac{k_{hn}}{k_f} = \left\{ \frac{k_1\varphi_1 + k_2\varphi_2}{\varphi_1 + \varphi_2} + 2k_f + 2(k_1\varphi_1 + k_2\varphi_2) - 2(\varphi_1 + \varphi_2)k_f \right\} \times \left\{ \frac{k_1\varphi_1 + k_2\varphi_2}{\varphi_1 + \varphi_2} + 2k_f - 2(k_1\varphi_1 + k_2\varphi_2) + (\varphi_1 + \varphi_2)k_f \right\}^{-1} \quad (9)$$

The dynamic viscosity of a hybrid nanofluid as follows: (Mabood et al. [26])

$$\mu_{hnf} = \frac{\mu_f}{(1 - \varphi_1)^{2.5}(1 - \varphi_2)^{2.5}} \quad (10)$$

The boundary conditions of natural convection in dimensionless form are listed in the following Table 2.

**Table 2.** Hydrodynamic and thermal boundary conditions.

Limit	Hydrodynamic Conditions	Thermal Conditions
Left wall $0 < Y < 1, X = 0$	$U = V = 0$	$\theta = 1$
Right wall $0 < Y < 1, X = 1$	$U = V = 0$	$\theta = 0$
Upper wall $0 < X < 1, Y = 1$	$U = V = 0$	$\frac{d\theta}{dY} = 0$
Lower wall $0 \leq X \leq 1, Y = 0$	$U = V = 0$	$\frac{\partial \theta}{\partial y} = 0$

The reduced variables used during the dimensioning of equations (1-4) as well as the Prandtl, Grashof and Rayleigh numbers are respectively given by the following expressions:

$$X = \frac{x}{H}, \quad Y = \frac{y}{H}, \quad U = \frac{u}{(a/L)}, \quad V = \frac{v}{(a/L)}, \quad P = \frac{P}{\rho \left( \frac{a}{L} \right)^2}, \quad \theta = \frac{T - T_c}{T_h - T_c} \quad (11)$$

$$Gr = \frac{g\beta_f(T_h - T_c)H^3}{\nu_f^2}, \quad Pr = \frac{\nu_f}{\alpha_f}, \quad Ra = Gr \cdot Pr \quad (12)$$

By carrying the dimensionless quantities defined above in the equations of the mathematical model (1), (2), (3), and (4), we obtain:

$$\frac{\partial U}{\partial X} + \frac{\partial V}{\partial Y} = 0 \quad (13)$$

$$U \frac{\partial U}{\partial X} + V \frac{\partial U}{\partial Y} = -\frac{\partial P}{\partial X} + Pr \left( \frac{\partial^2 U}{\partial X^2} + \frac{\partial^2 U}{\partial Y^2} \right) \quad (14)$$

$$U \frac{\partial V}{\partial X} + V \frac{\partial V}{\partial Y} = -\frac{\partial P}{\partial Y} + Pr \left( \frac{\partial^2 V}{\partial X^2} + \frac{\partial^2 V}{\partial Y^2} \right) + Ra \cdot Pr \cdot \theta \quad (15)$$

$$U \frac{\partial \theta}{\partial X} + V \frac{\partial \theta}{\partial Y} = \left( \frac{\partial^2 \theta}{\partial X^2} + \frac{\partial^2 \theta}{\partial Y^2} \right) \quad (16)$$

The local Nusselt number (Nu) along the lower hot wall can be expressed by:

$$Nu = -\frac{k_{nf}}{k_f} \cdot \frac{\partial \theta / \partial n}{T_h - T_c} \cdot H \quad (17)$$

The average value of the Nusselt number along this wall is calculated by the following integral:

$$\overline{Nu} = \frac{1}{H} \int_0^H \frac{k_{nf}}{k_f} \left\{ \left| \frac{\partial \theta}{\partial Y} \right|_{Y=0} \right\} dX \quad (18)$$

### 3. Numerical Method

To solve the equations governing this problem, we employed the SIMPLE algorithm along with the second-order scheme of the finite volume method. The computations were carried out using the Ansys-Fluent 6.3 software.

#### 3.1. Mesh independence

A quadratic cell mesh is utilized for this study. The mesh is meticulously designed to refine near the block and adjacent walls, gradually coarsening as it extends farther away from both. The objective of this approach is to decrease the total computational expense while improving the accuracy of the simulation outcomes. To examine the impact of node count, four distinct meshes with 175x175, 200x200, 225x225, and 300x300 nodes are chosen, enabling the attainment of highly accurate solutions without compromising computational time. The average Nusselt number obtained using different grids for particular cases is presented in Table 3. As can be seen from this table, a 200x200 grid is fine enough for the numerical calculation performed in the current project.

**Table 3.** Flow characteristics for different grids.

Mesh	175x175	200x200	225x225	300x300
$Nu_{avg}$	5.914798	5.906531	5.90402	5.90368

#### 3.2. Code validation

To validate the simulation code, we conducted a comparative analysis by comparing the current results with those reported by Takabi, B et al. [27]. This comparison focused on a sinusoidal cavity with a discrete heat source on the bottom wall. Takabi and others studied laminar natural convection with Al<sub>2</sub>O<sub>3</sub>/H<sub>2</sub>O nanofluid and Al<sub>2</sub>O<sub>3</sub>-Cu/H<sub>2</sub>O hybrid nanofluid in a range of conditions. The specific case compared involved Rayleigh numbers of  $Ra=10^3$  and  $Ra=10^5$ , with a nanoparticle volume fraction  $\phi=1\%$ . Figure 2 illustrates the isotherms for both studies, showcasing excellent agreement between the present simulation and the previous results. The results show that the numerical method used here can accurately describe how heat moves through sinusoidal cavities, especially when hybrid nanofluids are present.

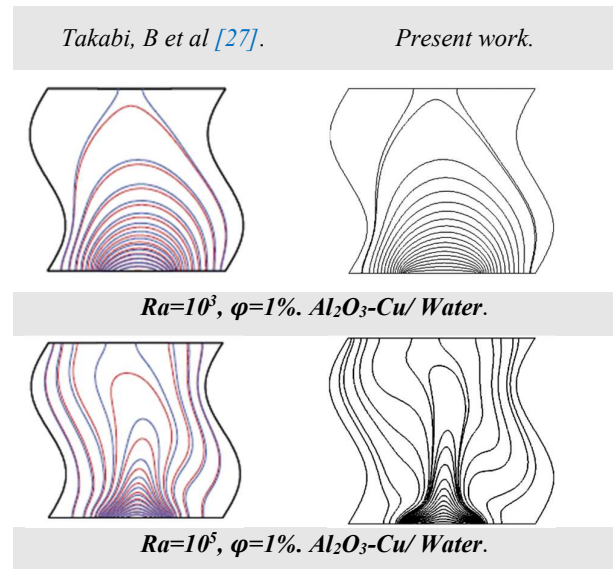


**Figure 2.** Isotherm comparison.

The second validation case in this study comes from a well-known issue with nanofluids naturally convecting in a two-dimensional cavity with wavy walls, which was looked into by Boulahia, Z. et al. [28]. Analyzed two configurations: one with a wavy cavity that maintains the vertical walls at different temperatures, and another with a wavy cavity that features a centrally placed cooler and heated vertical walls. We assumed the nanofluid to be Newtonian, incompressible, and laminar, maintaining thermal equilibrium conditions throughout the cavity. We used the average Nusselt number as a key performance metric for this validation. Figures 3 and Figure 4 show a direct comparison between the results of the current study and the numerical data obtained by Boulahia et al. [28] using Fluent 6.3. The excellent agreement observed in these figures underscores the accuracy and reliability of the present numerical model, further confirming the validity of the simulation procedures employed. This validation process reveals the robustness of the simulation framework in this study, which delivers highly accurate predictions of heat transfer characteristics in wavy-wall cavities. The agreement with both experimental and numerical results from previous studies not only proves that the methods used are correct, but it also shows how useful it is to use hybrid nanofluids, especially Al<sub>2</sub>O<sub>3</sub>-Cu/H<sub>2</sub>O, to improve thermal performance in complicated shapes. These findings are essential for optimizing designs where natural convection plays a critical role,

especially in systems involving corrugated walls and hybrid nanofluid applications.

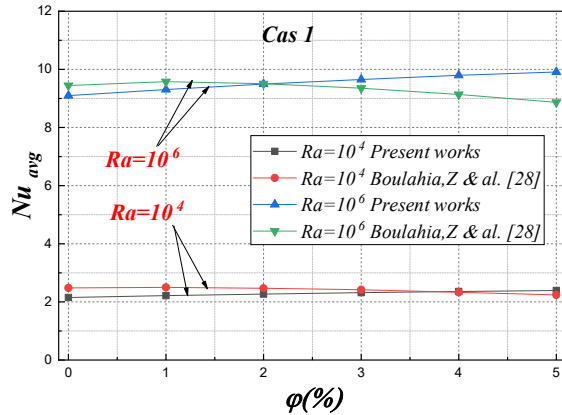


**Figure 3.** Evolution of the average Nusselt number along the hot wall for different volume fractions.

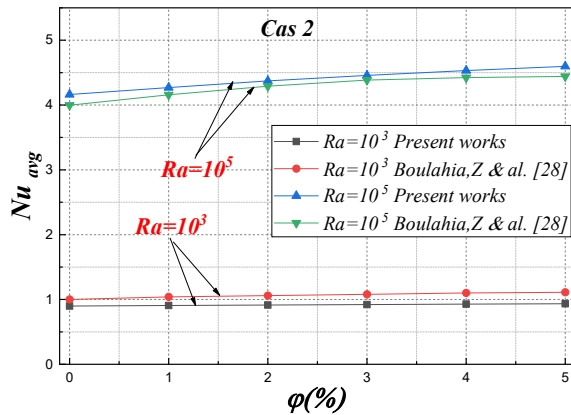


**Figure 4.** Evolution of the average Nusselt number along the hot wall for different volume fractions.

## 4. Results and Discussion

In this study, we examine the laminar natural convection flow in a cavity with sinusoidal undulated walls, focusing on the hydrodynamic behavior and heat transfer characteristics when two distinct nanoparticles are incorporated into a base fluid. The cavity is heated via a heat source positioned on the left wall, and the effects of Rayleigh number (ranging from  $10^3 \leq Ra \leq 10^6$  and hybrid nanofluid concentration (volumetric concentration between 0% and 6%) on both heat transfer and hydrodynamic performance were thoroughly analyzed. This analysis was conducted by evaluating the thermal and dynamic fields, as well as the temperature and velocity profiles along the longitudinal and transverse midsections of the enclosure.

### 4.1. Influence of nanoparticle concentration and Rayleigh number

Figure 5 displays temperature contours for Rayleigh numbers ranging from  $10^3$  to  $10^6$ . As observed, heat from the hot source is transported upward via convection within the enclosure. A fairly uniform distribution of heat is noted across both sidewalls, with slight tilts in the isotherms at  $Ra=10^3$ , signifying the onset of convection.

For Rayleigh numbers below  $Ra=10^4$ , the intensity of convection inside the cavity remains low, with viscous forces dominating buoyancy forces. Under these conditions, diffusion remains the primary mode of heat transfer, as noted by Saha, G. [29] and Hussain, S. et al. [30]. The isotherm profiles remain similar to those observed in conduction-dominated heat transfer models, showing minimal variation until  $Ra=10^4$ .

At higher Rayleigh numbers, the increasing convection intensity results in significant modifications to the isotherm model, reflecting a shift towards convection-dominated heat transfer within the cavity. The shape of the isotherms is significantly influenced by the Rayleigh number, particularly at  $Ra=10^5$  and  $Ra=10^6$ , where the isotherms become predominantly horizontal in the middle of the enclosure. The increased Rayleigh number, in combination with larger exchange surfaces, significantly affects the heat transfer mode, with convective motion beginning at  $Ra=10^5$  and becoming dominant at  $Ra=10^6$ .

The results indicate that heat exchange within the cavity increases with higher Rayleigh numbers and an increase in the number of wall undulations. The thermal flow is concentrated near the active isothermal vertical walls, as evidenced by the increasingly tight isotherms with rising Rayleigh numbers. The central part of the cavity remains almost thermally homogeneous, allowing us to predict the direction of recirculation vortices, which rotate clockwise. Additionally, the isotherms stay perpendicular to the adiabatic walls due to the boundary conditions, where the temperature gradient is zero at these walls. As both the number of wall undulations and the Rayleigh number increase, the distortion of isotherms becomes more pronounced, particularly with the inclusion of nanoparticles. The cavity's undulated configuration plays a critical role in influencing both flow structure and heat transfer.



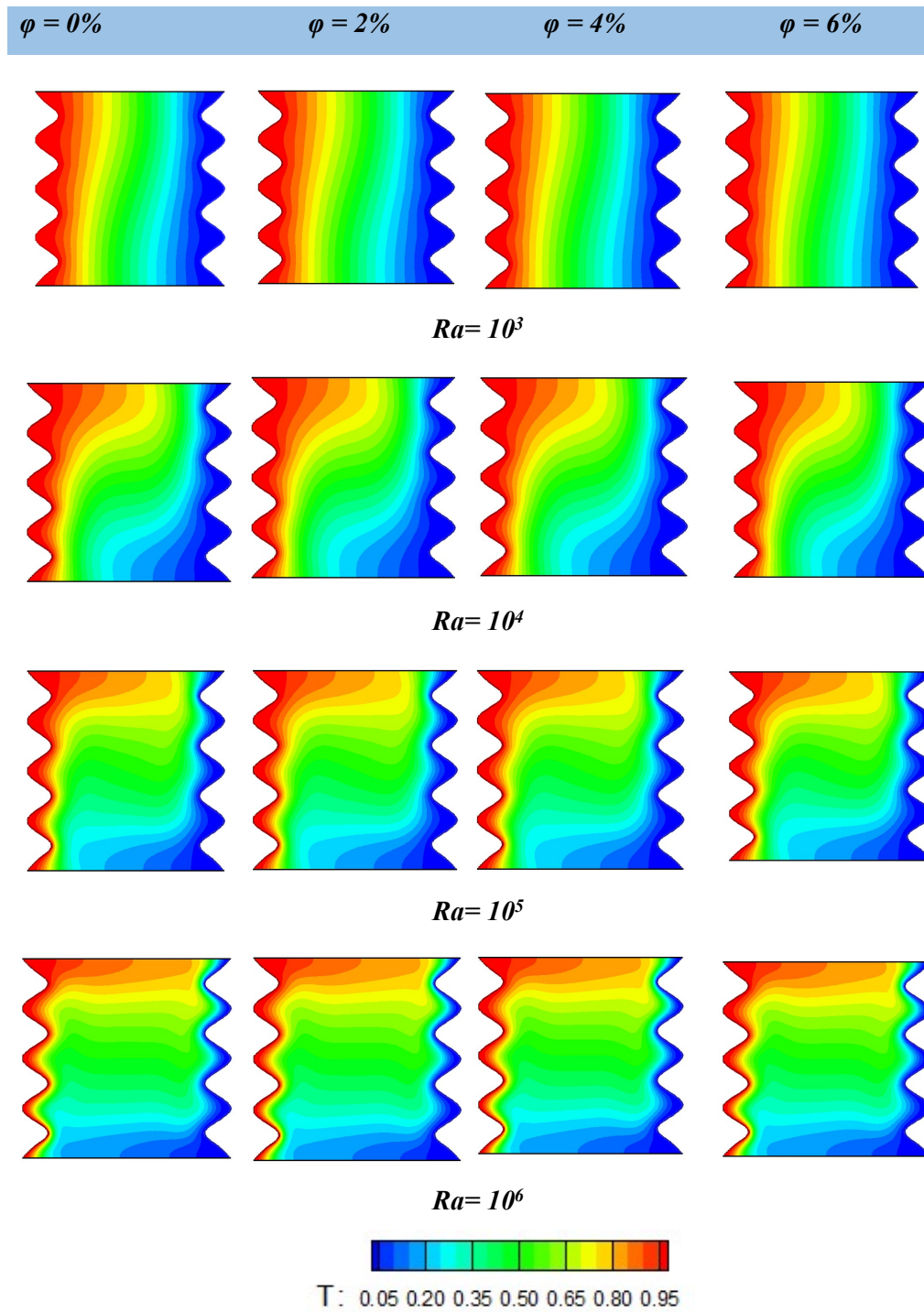


**Figure 5.** The contours of the isotherms of the hybrid nanofluid *Ag-CuO/Water*, for different Rayleigh numbers ( $Ra$ ) and volume fractions.

#### 4.1.1. Temperature profiles and heat transfer mechanism

Figures 6(a) and 6(b) present the temperature profiles along the vertical and horizontal midlines within the enclosure (at  $y = 0.5H$  and  $x = 0.5L$ , respectively) for different Rayleigh numbers using a 4% volume fraction of Ag-CuO/water hybrid nanofluid.

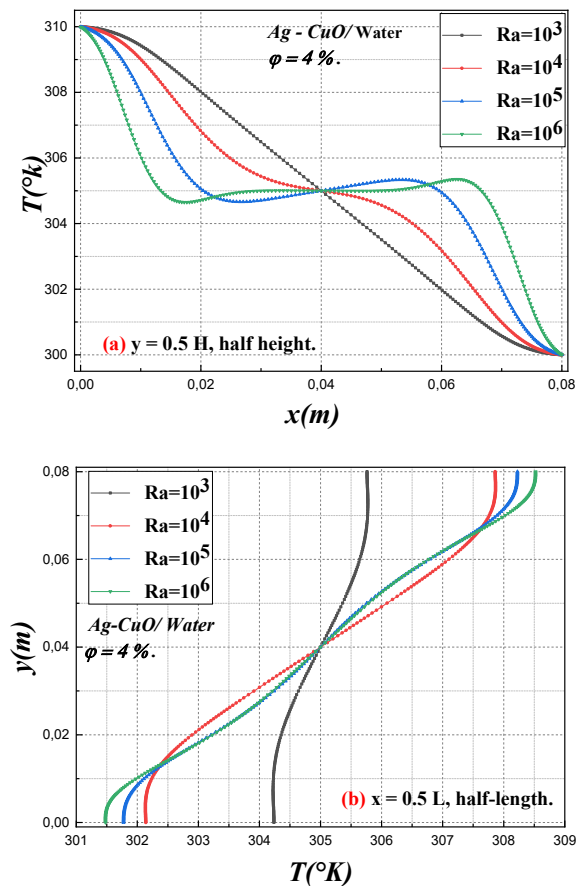


**Figure 6.** Temperature profile along the cavity mid planes for different Rayleigh numbers.

The profiles demonstrate a shift in heat transfer mechanisms, transitioning from conduction to convection as the Rayleigh number increases. At  $Ra=10^3$ , the temperature profile follows a linear negative slope, characteristic of a purely conductive regime where the fluid acts like a solid, transmitting heat through conduction. As buoyancy forces remain insufficient to overcome viscosity, the fluid particles remain mostly stationary, with heat transfer occurring solely via conduction. However, at higher Rayleigh numbers, the

temperature profiles reveal nonlinear behavior, indicating the increasing influence of convection. The thermal buoyancy forces drive this change, intensifying heat transfer as  $Ra$  increases. Interestingly, the vertical midline temperature distribution becomes less sensitive to the presence of nanoparticles as convection intensifies.

#### 4.1.2. Dynamic field and streamline contours

Figure 7 illustrates the streamline contours for different Rayleigh numbers and varying volume fractions of the Ag-CuO/water hybrid nanofluid. Differences between the pure fluid and the hybrid nanofluid are attributed to the higher viscosity of the hybrid nanofluid, which increases momentum diffusion.

A rotating cell forms, rotating slowly in a clockwise direction due to the buoyancy-driven upward movement of fluid particles along the hot left wall and downward movement along the cold right wall. For  $Ra \geq 10^4$ , significant changes in isoconcentration structures are observed, with deformation aligning with the streamlines' rotation. Convective heat transfer becomes prominent as stream function values increase.

At lower Rayleigh numbers ( $Ra \leq 10^4$ ), the flow remains single-celled, occupying most of the cavity, and as  $Ra$  increases, the streamlines deform from circular to elliptical shapes. At  $Ra=10^5$ , the streamlines exhibit symmetry about the cavity's center, with their intensity decreasing towards the center.

Further analysis reveals that the presence of nanoparticles does not significantly affect the velocity distribution profiles, though a slight decrease in streamline intensity is noted in comparison to pure water. This result aligns with findings by Abu-Nada, E. et al. [31], which suggest that nanoparticles increase viscous drag, slowing fluid motion within the cavity. However, the Rayleigh number continues to exert a more substantial effect, particularly in the cavity's central region, a result consistent with the work of Nasrin, R. et al. [32].



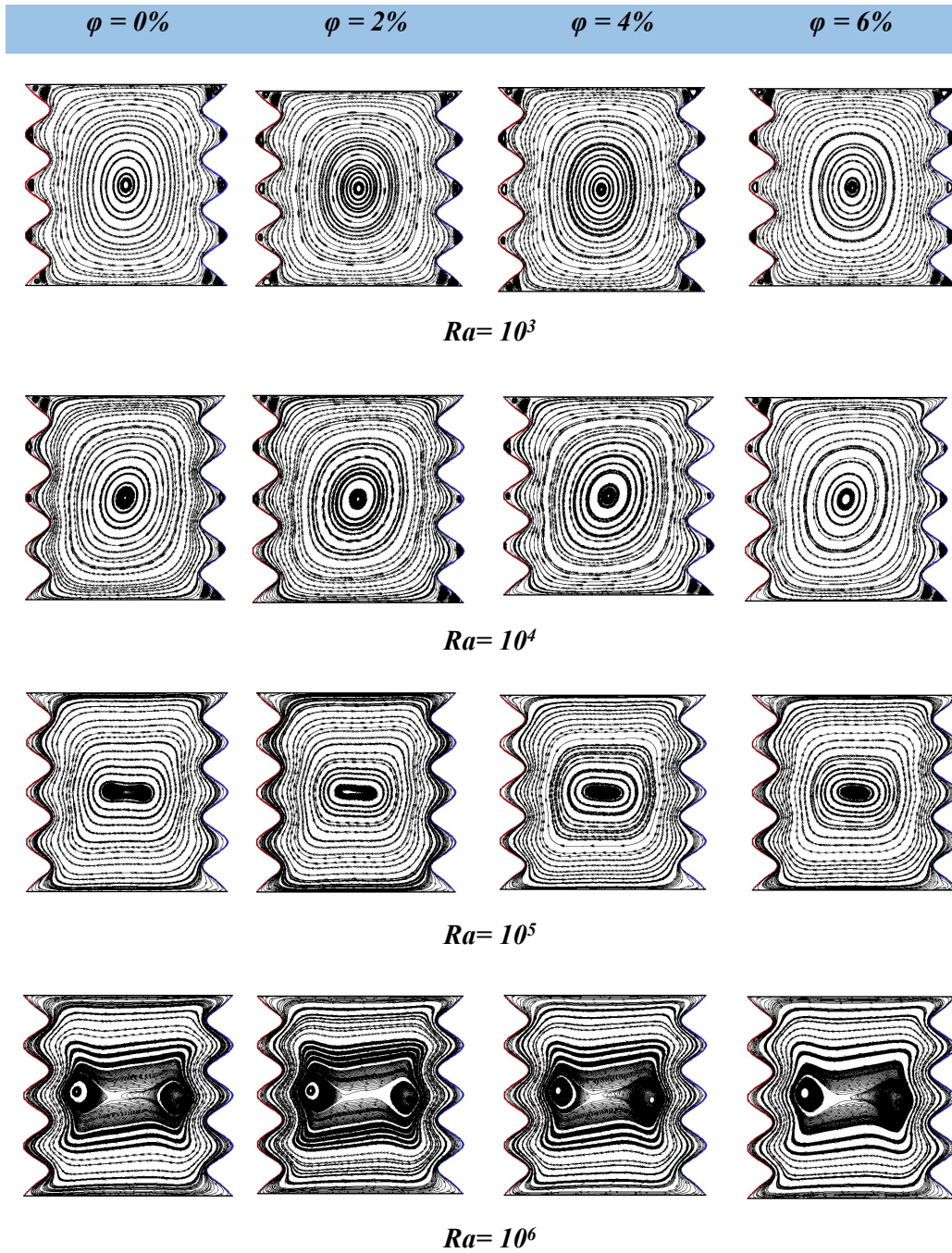


**Figure 7.** The contours of the current lines in the cavity (*Ag-CuO / Water*), for different Rayleigh numbers ( $Ra$ ) and different volume fractions.

#### 4.1.3. Velocity profiles

Figures 8(a) and 8(b) illustrate the transverse and longitudinal velocity profiles within the cavity, respectively. The profiles exhibit symmetry around the cavity center, with both horizontal and vertical velocity components demonstrating a typical natural convection pattern. At  $Ra=10^3$ , both velocity components are nearly zero, indicating a purely conductive heat transfer regime. As  $Ra$  increases, the upward and downward fluid motion intensifies near the vertical walls, with velocity profiles peaking at  $Ra=10^6$ , particularly near the wall regions. This behavior is consistent with the increasing influence of convection as  $Ra$  rises.

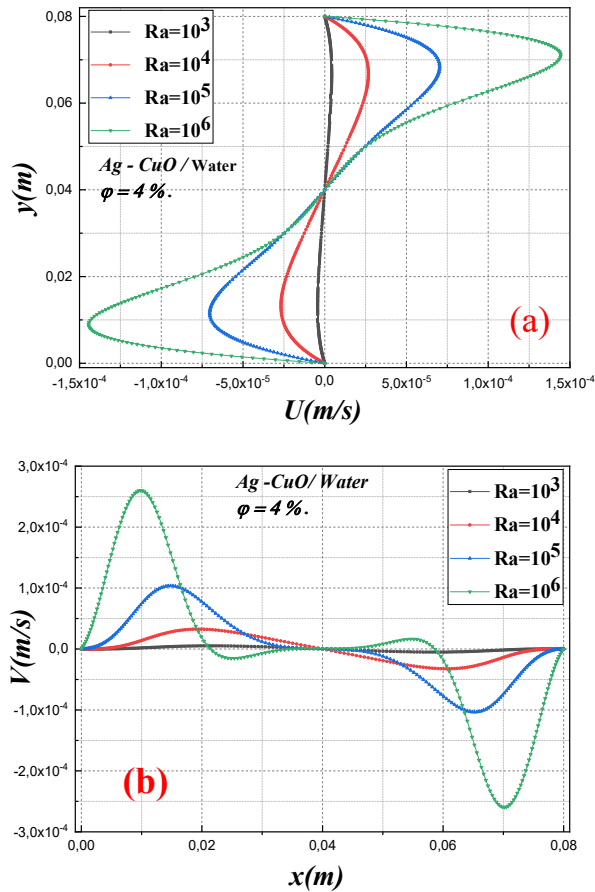


**Figure 8.** Transverse and longitudinal velocity profiles for different Rayleigh numbers.

##### 1.1.1. Heat Transfer and Nusselt Number Variation

Figure 9 displays the variation of the average Nusselt number along the heated left wall for both pure water and

the Ag-CuO/water hybrid nanofluid at various nanoparticle concentrations. As expected, the average Nusselt number increases with higher Rayleigh numbers, but a slight decrease is observed with increasing nanoparticle volume fractions. This reduction is likely due to the simultaneous increase in fluid viscosity and thermal conductivity, which limits convective heat transfer under low convection conditions.

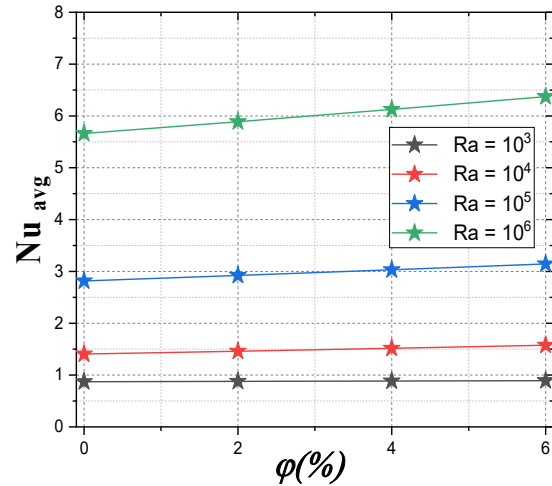


**Figure 9.** Variation of the Nusselt number in the function of volume fractions for different numbers of Rayleigh  $Ra$ .

Additionally, Figure 10 shows the relationship between the average Nusselt number and Rayleigh number for different volumetric fractions.

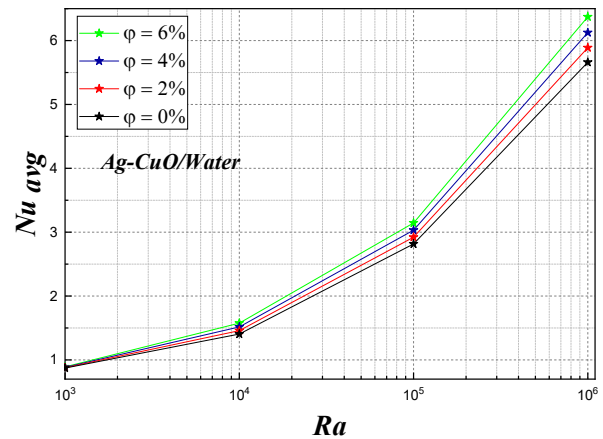


**Figure 10.** Variation of the average Nusselt number for the different Rayleigh numbers.

The results confirm that the average Nusselt number increases more substantially at higher Rayleigh numbers, driven by the intensification of buoyancy forces and the resulting thermal diffusion exchanges between the nanoparticles. The enhancement of thermal performance using Ag-CuO/water hybrid nanofluid is particularly notable compared to both pure water and the individual Ag/water and CuO/water nanofluids, underscoring the benefits of higher nanoparticle concentrations in improving heat transfer.

#### 4.2. The effect of the wavy shape of the wall

As shown in Figure 5, it is evident that adding protrusions to the cavity wall significantly enhances heat transfer by altering fluid flow patterns and improving convective heat transfer. The increase in surface area and changes in flow behavior contribute to more effective heat dissipation. Furthermore, the fluid flowing around the protrusions experiences variations in velocity and direction, promoting enhanced mixing. This increased mixing, caused by the presence of the protrusions, facilitates better thermal interaction between the fluid and the wall surface, thereby improving heat transfer efficiency. The presence of protrusions disrupts the development of thermal boundary layers near the wall.

Boundary layers, which are thin layers of fluid adjacent to the surface, can hinder heat transfer. Disrupting these layers allows cooler fluid to make contact with the surface, leading to more efficient heat transfer. Additionally, the shape of the protrusions can induce the formation of secondary flow patterns within the fluid. By adding protrusions to the cavity, the effective surface area is increased, boundary layers are disrupted, and secondary flows are encouraged, all of which collectively enhance convective heat transfer and improve heat dissipation from the surface. The flow and temperature fields across the free surface pass through the vertices, with a minimum between them. The maximum limits of the fluid parameters on the free surface increase due to the shape functions of the protrusions. Overall, the heat transfer in a cavity with sinusoidal walls is greater than in a cavity with vertical, uniform walls of the same size.

At the apex, streamlines approach the wall just after the peak. The temperature distribution in this region exhibits the same characteristics as shown in Figure 7, which explains the decrease in the thickness of the thermal boundary layer after the apex. In the middle of the cavity, the flow remains laminar. Under the influence of the corrugation, the thickness of the boundary layer first increases and then decreases. It is evident that the shape of the flow cells is influenced by the corrugated wall, as seen in various graphs. Heat transfer can also be improved by adding protrusions on the wall to increase the total surface area. Finally, it can be concluded that sinusoidal protrusions enhance heat transfer, meaning that the shape of the protruding surfaces plays a significant role compared to a smooth surface (Figure 7).

#### 4.3. Critical study and comparison of obtained results

##### 4.3.1. Effect of Rayleigh number on temperature distribution

Results Obtained: At low Rayleigh numbers ( $Ra \leq 104$ ), the temperature distribution is typical of a low thermal gradient. This indicates that the buoyant convection is not sufficient to overcome the viscosity, and heat transfer remains by conduction. As the Rayleigh number increases to 105 and 106, the intensity of convection increases significantly, which enhances the efficiency of convective heat transfer. Comparisons with other studies: These results are consistent with what Parvin et al. [33] and Hasan, M.N et al. [34] reported, who showed that convection is the dominant mechanism at higher Rayleigh numbers. However, this study featured hybrid nanoparticles, which further affected the thermal distribution compared to conventional studies that used only base fluids.

##### 4.3.2. Impact of nanoparticles on convective flow and aerodynamic properties.

The findings showed that adding Ag-CuO/water nanoparticles changes how the streamlines are distributed and how the flow behaves inside the cavity. Multiple vortex cells form at high Rayleigh numbers, allowing the streams to move more freely than in the baseline case. The nanoparticles generate a slight decrease in the intensity of the velocity lines. Comparisons with other studies:

Kadhim, H. T et al. [35], who reported the effect of nanoparticles on aerodynamics, observed similar results. However, the present study differs in providing detailed analyses of the effects of nanoparticles with different compositions. This enhances our understanding of how to improve the performance of convection systems using hybrid nanofluids

## 5. Conclusion

In this parametric numerical study, laminar natural convection and heat transfer in a cavity with opposing undulated walls saturated with a hybrid Ag-CuO/water nanofluid were investigated. The study explored the effects of sinusoidally undulated wall geometry, different volume fractions of nanoparticles ( $0\% \leq \phi \leq 6\%$ ), and Rayleigh numbers ( $10^3 \leq Ra \leq 10^6$ ). The finite-volume discretization method was employed to solve the governing equations.

The results revealed that an increase in the volumetric fraction of nanoparticles enhanced the heat exchange rate in the cavity. The Rayleigh number significantly influenced the dominant heat transfer mode, especially with increased surface area. Additionally, an increase in the number of wall undulations led to a reduction in the heat transfer rate.

Several key observations were made regarding temperature profiles, streamlines, and velocity components. At lower  $Ra$ , the heat transfer was mainly conductive, transitioning to convective as  $Ra$  increased. The addition of nanoparticles affects temperature distributions, with notable effects on streamlines and velocity profiles. The study also showed that the hybrid nanofluid (Ag-CuO/water) outperformed pure water and individual nanofluids (Ag/water and CuO/water) due to the increasing volume fraction of silver nanoparticles. The increased thermal conductivity of the hybrid nanofluid contributed to improved heat transfer.

In conclusion, this research contributes to the understanding of thermal and fluidic behavior in undulated cavities with hybrid nanofluids. The findings have implications for optimizing heat transfer in various applications, from industrial processes to domestic heating systems, by leveraging the unique properties of nanofluids.

## Nomenclature

$A$	wavy surface amplitude
$C$	Heat capacity ( $J/m^3 \cdot K$ )
$C_p$	Specific heat ( $J/kg \cdot K$ )
$k$	Thermal conductivity ( $W/m \cdot K$ )
$T$	Temperature (K)
$g$	Gravitational acceleration ( $m/s^2$ )
$H$	Cavity length
$k$	Thermal conductivity ( $W/m \cdot K$ )
$n$	Number of undulations
$Nu$	Local Nusselt Number
$Nu_{avg}$	Average Nusselt number
$Pr$	Prandtl number
$Ra$	Rayleigh number
$U, V$	Nondimensional velocities in the $x$ - and $y$ -direction
$u, v$	Velocities in the $x$ - and $y$ -direction ( $m/s$ )
$X, Y$	Nondimensional coordinates

## Greek Symbols

$\alpha$	thermal diffusivity ( $m^2/s$ )
$\beta$	Buoyancy coefficient ( $K^{-1}$ )
$\theta$	Non-dimensional temperature
$\mu$	Dynamic viscosity ( $Kg/m \cdot s$ )
$\nu$	The kinematic viscosity ( $m^2/s$ )
$\rho$	Density ( $kg/m^3$ )
$\phi$	Volume fraction of nanoparticles

## Subscripts

$c$	Cold
$h$	Hot
$hnf$	Hybrid nanofluid

### Competing Interest Statement

The authors declare no known competing financial interests or personal relationships that could have influenced the work reported in this paper.

### Data and Materials Accessibility

No data or additional materials were utilized for the research described in the article.

### Author Contribution Roles

We would like to point out that all authors contributed equally to all phases of this research. Each co-author actively participated in the conceptualization, methodology, validation of results, data analysis, and writing and revision of the manuscript. Thus, we wish to emphasize that all stages of the research and publication process were carried out in close collaboration, without major distinction in individual responsibilities.

### References

- [1] J.C. Maxwell, *A Treatise on Electricity and Magnetism*, vol. 1, Clarendon Press, 1873.
- [2] J.C. Maxwell, *A Treatise on Electricity and Magnetism*, 2nd ed., Oxford University Press, Cambridge, UK, 1881.
- [3] S.U. Choi and J.A. Eastman, "Enhancing thermal conductivity of fluids with nanoparticles," Argonne National Lab., Argonne, IL, 1995, No. ANL/MSD/CP-84938, CONF-951135-29. [Online]. Available: [https://scholar.google.com/scholar\\_lookup?title=Enhancing%20thermal%20conductivity%20of%20fluids%20with%20nanoparticles&publication\\_year=1995&author=S.U.%20Choi&author=J.%20Eastman](https://scholar.google.com/scholar_lookup?title=Enhancing%20thermal%20conductivity%20of%20fluids%20with%20nanoparticles&publication_year=1995&author=S.U.%20Choi&author=J.%20Eastman)
- [4] J.A. Eastman, S.U.S. Choi, S. Li, W. Yu, and L.J. Thompson, "Anomalously increased effective thermal conductivities of ethylene glycol-based nanofluids containing copper nanoparticles," *Applied Physics Letters*, vol. 78, no. 6, pp. 718–720, 2001, doi: <https://doi.org/10.1063/1.1341218>.
- [5] S. Suresh, K.P. Venkitaraj, P. Selvakumar, and M. Chandrasekar, "Synthesis of Al<sub>2</sub>O<sub>3</sub>-Cu/water hybrid nanofluids using two-step method and its thermo-physical properties," *Colloids and Surfaces A: Physicochemical and Engineering Aspects*, vol. 388, no. 1–3, pp. 41–48, 2011, doi: <https://doi.org/10.1016/j.colsurfa.2011.08.005>.
- [6] S. Ostrach, "Natural convection in enclosures," *J. Heat Transfer*, vol. 110, no. 4b, pp. 1175–1190, 1988, doi: <https://doi.org/10.1115/1.3250619>.
- [7] J.L. Lage and A. Bejan, "Natural convection from a vertical surface covered with hair," *International Journal of Heat and Fluid Flow*, vol. 12, no. 1, pp. 46–53, 1991, doi: [https://doi.org/10.1016/0142-727X\(91\)90007-I](https://doi.org/10.1016/0142-727X(91)90007-I).
- [8] A.J.N. Khalifa, "Natural convective heat transfer coefficient—a review: I. Isolated vertical and horizontal surfaces," *Energy Conversion and Management*, vol. 42, no. 4, pp. 491–504, 2001, doi: [https://doi.org/10.1016/S0196-8904\(00\)00042-X](https://doi.org/10.1016/S0196-8904(00)00042-X).
- [9] M. Ali, "Natural convection heat transfer in a square duct with v-corrugated vertical walls," *Journal of Energy Heat and Mass Transfer*, vol. 14, pp. 125–131, 1992.
- [10] M. Ali and M.N. Ali, "Finite element analysis of laminar convection heat transfer and flow of the fluid bounded by V-corrugated vertical plates of different corrugation frequencies," 1994. [Online]. Available: <https://nopr.niscpr.res.in/handle/123456789/29956>.
- [11] S. Noorshahi, C.A. Hall III, and E.K. Glakpe, "Natural convection in a corrugated enclosure with mixed boundary conditions," 1996, doi: <https://doi.org/10.1115/1.2847946>.
- [12] M. Ali and S.R. Husain, "Effect of corrugation frequencies on natural convective heat transfer and flow characteristics in a square enclosure of vee-corrugated vertical walls," *International Journal of Energy Research*, vol. 17, no. 8, pp. 697–708, 1993, doi: <https://doi.org/10.1002/er.4440170804>.
- [13] E. Abu-Nada and H.F. Oztog, "Numerical analysis of Al<sub>2</sub>O<sub>3</sub>/water nanofluids natural convection in a wavy-walled cavity," *Numerical Heat Transfer, Part A: Applications*, vol. 59, no. 5, pp. 403–419, 2011, doi: <https://doi.org/10.1080/10407782.2011.552363>.
- [14] H.F. Oztog, E. Abu-Nada, Y. Varol, and A. Chamkha, "Natural convection in wavy enclosures with volumetric heat sources," *International Journal of Thermal Sciences*, vol. 50, no. 4, pp. 502–514, 2011, doi: <https://doi.org/10.1016/j.ijthermalsci.2010.10.015>.
- [15] Y. Asako and M. Faghri, "Finite-volume solutions for laminar flow and heat transfer in a corrugated duct," 1987, doi: <https://doi.org/10.1115/1.3248134>.
- [16] G. Fabbri, "Heat transfer optimization in corrugated wall channels," *International Journal of Heat and Mass Transfer*, vol. 43, no. 23, pp. 4299–4310, 2000, doi: [https://doi.org/10.1016/S0017-9310\(00\)00054-5](https://doi.org/10.1016/S0017-9310(00)00054-5).
- [17] L. Goldstein Jr. and E.M. Sparrow, "Heat/mass transfer characteristics for flow in a corrugated wall channel," 1977, doi: <https://doi.org/10.1115/1.3450667>.

- [18] G. Saha, "Finite element simulation of magnetoconvection inside a sinusoidal corrugated enclosure with discrete isoflux heating from below," *International Communications in Heat and Mass Transfer*, vol. 37, no. 4, pp. 393–400, 2010, doi: <https://doi.org/10.1016/j.icheatmasstransfer.2009.12.001>.
- [19] S.H. Hussain, A.K. Hussein, and R.N. Mohammed, "Studying the effects of a longitudinal magnetic field and discrete isoflux heat source size on natural convection inside a tilted sinusoidal corrugated enclosure," *Computers & Mathematics with Applications*, vol. 64, no. 4, pp. 476–488, 2012, doi: <https://doi.org/10.1016/j.camwa.2011.12.022>.
- [20] E. Abu-Nada and A.J. Chamkha, "Effect of nanofluid variable properties on natural convection in enclosures filled with a CuO–EG–Water nanofluid," *International Journal of Thermal Sciences*, vol. 49, no. 12, pp. 2339–2352, 2010, doi: <https://doi.org/10.1016/j.ijthermalsci.2010.06.013>.
- [21] A.J. Chamkha, H.F. Oztop, and M.A. Mansour, "Effects of nanofluid variable properties on mixed convection in lid-driven enclosures partially heated from a corner," *International Communications in Heat and Mass Transfer*, vol. 37, no. 8, pp. 1157–1165, 2010, doi: <https://doi.org/10.1016/j.icheatmasstransfer.2010.07.003>.
- [22] H.F. Oztop, E. Abu-Nada, and I. Pop, "Numerical analysis of mixed convection in a lid-driven cavity partially heated from below using nanofluids," *European Journal of Mechanics - B/Fluids*, vol. 29, no. 5, pp. 563–573, 2010, doi: <https://doi.org/10.1016/j.euromechflu.2010.04.007>.
- [23] R. Nasrin and M.A. Alim, "Prandtl number effects on unsteady mixed convection in a lid-driven cavity with a wavy bottom surface," *International Journal of Heat and Fluid Flow*, vol. 38, pp. 29–41, 2012, doi: <https://doi.org/10.1016/j.ijheatfluidflow.2012.05.005>.
- [24] Y. Varol, H.F. Oztop, and I. Pop, "Numerical analysis of natural convection in a square enclosure with a wavy wall filled with nanofluids," *International Communications in Heat and Mass Transfer*, vol. 38, no. 5, pp. 571–577, 2011, doi: <https://doi.org/10.1016/j.icheatmasstransfer.2011.02.015>.
- [25] H.F. Oztop, E. Abu-Nada, and A.J. Chamkha, "Natural convection in wavy enclosures using nanofluids," *European Journal of Mechanics - B/Fluids*, vol. 29, no. 5, pp. 685–695, 2010, doi: <https://doi.org/10.1016/j.euromechflu.2010.04.006>.
- [26] H.F. Oztop, I. Pop, and A.J. Chamkha, "Numerical study of heat transfer by natural convection in a cavity with a sinusoidal wall," *International Communications in Heat and Mass Transfer*, vol. 37, no. 5, pp. 587–595, 2010, doi: <https://doi.org/10.1016/j.icheatmasstransfer.2010.03.007>.
- [27] K.M. Pandey, M. Manohar, and S. Shukla, "Numerical simulation of fluid flow and heat transfer using Cu and Ag based nanofluids in a wavy enclosure," *Journal of Mechanical Science and Technology*, vol. 32, no. 2, pp. 849–860, 2018, doi: <https://doi.org/10.1007/s12206-018-0136-7>.
- [28] B.M. Taslim and S. Vafai, "Mixed convection in cross-corrugated ducts," *Numerical Heat Transfer, Part A: Applications*, vol. 24, no. 2, pp. 245–265, 1993, doi: <https://doi.org/10.1080/1040778930891362>.
- [29] P. Selvakumar and S. Suresh, "Convective heat transfer coefficient and friction factor of silver/water nanofluid in a circular tube: Experimental data and theoretical approach," *International Journal of Heat and Mass Transfer*, vol. 55, no. 11–12, pp. 2761–2768, 2012, doi: <https://doi.org/10.1016/j.ijheatmasstransfer.2012.01.069>.
- [30] M. Hatami and D.D. Ganji, "Thermal and flow analysis of boundary layer passing through a permeable stretching/shrinking wedge," *Case Studies in Thermal Engineering*, vol. 4, pp. 59–66, 2014, doi: <https://doi.org/10.1016/j.csite.2014.07.001>.
- [31] E. Abu-Nada, H.F. Oztop, and Y. Varol, "Mixed convection heat transfer in a lid-driven cavity with a wavy wall using nanofluids," *Numerical Heat Transfer, Part A: Applications*, vol. 58, no. 6, pp. 499–518, 2010, doi: <https://doi.org/10.1080/10407782.2010.495181>.
- [32] I. Mahapatra and S. Kundu, "Analysis of natural convection in a square cavity with wavy walls using nanofluids," *Heat and Mass Transfer*, vol. 52, no. 2, pp. 357–368, 2016, doi: <https://doi.org/10.1007/s00231-015-1582-1>.
- [33] E. Abu-Nada and H.F. Oztop, "Effect of inclination angle on mixed convection in enclosures filled with Cu-water nanofluid," *International Journal of Heat and Fluid Flow*, vol. 30, no. 4, pp. 669–678, 2009, doi: <https://doi.org/10.1016/j.ijheatfluidflow.2009.03.007>.
- [34] S.K. Nayak, P.K. Singh, and B.K. Mishra, "Performance study of Cu–water nanofluid flow over a wavy surface," *Journal of Molecular Liquids*, vol. 220, pp. 670–678, 2016, doi: <https://doi.org/10.1016/j.molliq.2016.05.08>.
- [35] R. Nasrin and M.A. Alim, "Effects of magnetic field on natural convection in a wavy walled cavity with heat generation," *Engineering Science and Technology, an International Journal*, vol. 18, no. 3, pp. 443–454, 2015, doi: <https://doi.org/10.1016/j.jestech.2014.12.00>.
- [36] E.K. Gholinia, N. Alandjani, and E. Khodaverdi, "Magnetohydrodynamic mixed convection flow of a nanofluid in a cavity with a wavy wall," *Journal of Thermal Analysis and Calorimetry*, vol. 130, pp. 431–448, 2017, doi: <https://doi.org/10.1007/s10973-017-6400-2>.